



# 17. Uluslararası Yanma Sempozyumu

## 17<sup>th</sup> International Combustion Symposium

19-21 Eylül 2024, Prof. Dr. M. Mete Cengiz Kültür Merkezi / Bursa  
September 19<sup>th</sup> - 21<sup>st</sup> 2024, Prof. Dr. Mete Cengiz Congress and Convention Center / Bursa

**KONUŞMA ÖZETLERİ & BİLDİRİLER**  
**ABSTRACT & FULL TEXTS**



### Bilimsel İletişim

Dr. Öğr. Üyesi Merve Küçük Altay

Bursa Uludağ Üniversitesi

Mühendislik Fakültesi

Otomotiv Mühendisliği Bölümü

incos2024@yanmasempozyumu.com

[www.yanmasempozyumu.com](http://www.yanmasempozyumu.com)

Organizasyon Sekreteryası

**burken**  
TURİZM & KONGRE

444 9 443

onur.oral@burken.com

# **17. ULUSLARARASI YANMA SEMPOZYUMU**

## **17<sup>th</sup> INTERNATIONAL COMBUSTION SYMPOSIUM**

**19-21 Eylül 2024, Prof. Dr. M. Mete Cengiz Kültür Merkezi / Bursa**  
**September 19<sup>th</sup> – 21<sup>st</sup> Prof. Dr. M. Mete Cengiz Congress and Convention Center / Bursa**

### **BİLDİRİLER FULL TEXTS**

**ISBN: '978-625-6443-27-3'**

## **ABOUT THE COMBUSTION SYMPOSIUMS**

Combustion Symposiums, one of Turkey's longest-running and prestigious engineering symposium series, are organized as one of the periodic events of the Combustion Institute Turkey Branch. These symposiums, the first of which was held in 1983 and the 17th of which we plan to hold between 19-21 September 2024, were planned to be held in two-year periods. However, for various reasons, this schedule could not be adhered to and 16 symposiums were organized in 39 years. After the first five symposiums, all of which were held in Bursa, the symposium organization was opened to other universities. The other eight symposiums to date have been held at I.T.U., Gazi University, Marmara University, Kırıkkale University, Sakarya University, International University of Sarajevo (IUS), Kocaeli University, Erciyes University and Aydın Adnan Menderes University.

Combustion, as a thermo-chemical process that converts the chemical energy of fuels into heat or mechanical energy, has countless applications from domestic use to engines of transportation vehicles, from boilers to steel melting furnaces and power plants. Therefore, the technique and efficiency of this transformation are inherently important. Especially today, when energy has become a global strategic weapon, energy resources and how these resources can be used efficiently, and therefore fuels and combustion, are becoming an important area of interest in scientific research studies. The importance of the energy issue comes to the fore for countries that do not have sufficient energy resources, such as Turkey.

Combustion Symposiums are organizations that bring together academics and researchers who are experts on combustion from different countries, mostly from Turkey, and share their knowledge and studies on a common platform. Combustion Symposiums have been opened to international participation since the organization in 1993. The 11th Combustion Symposium, jointly organized by the International University of Sarajevo and Uludağ University, is the first symposium organized abroad.

We would be happy to have you among us as a sponsor or to contribute to the scientific objectives determined by the scope of the symposium.

BURKON is responsible for non-academic organizational activities. It will be sufficient to inform BURKON about your thoughts and decisions regarding scientific contribution and sponsorship.

Kind regards

**Prof. Dr. Ali SÜR MEN**  
**Symposium Chair**

**INDEX**

COMMITTEES .....	5
SCIENTIFIC PROGRAM.....	6
FULL TEXTS.....	12
ABSTRACT .....	281

September 19, 2024 Thursday

September 19, 2024 Thursday		
	A Salonu	B Salonu
	<p><b>Instrumentation of Piston Telemetry for Optimize Engine Operations</b> Elif Oral Öncül, F.B. Çevik, A.O. Özaslan, C. Cengiz and O. Erköse</p>	<p><b>Experimental Investigation on Regression Rate Behavior of Polylactic Acid in Hybrid Rocket Motor</b> Najihah Abd Razak, <u>Muhammad Hanafi Azami</u></p>
	<p><b>The Effect of the Olefin Composition in LPG on Autogas Conversion Systems</b> Mesut Barbaros, <u>Gizem Nur Ayan</u>, Emre Yılmaz</p>	<p><b>Comparative Evaluation of Syngas Mixtures for Gas Turbines</b> <u>Alp Kayaalp</u>, Hasan Kayhan Kayadelen</p>
12:15 - 14:00	<b>Öğle Yemeği</b>	
14:00 - 15:00	<p><b>Oturum Başkanı:</b> Levent Aydınbakar</p> <p><b>A New Era with Hydrogen and Future Directions for Better Environment and Sustainable Development</b> İbrahim Dinçer</p>	
15:00 - 16:40	<p><b>Sözel Bildiri Oturumu - 3</b> <b>Oturum Başkanı:</b> Zafer Gül</p>	<p><b>Sözel Bildiri Oturumu - 4</b> <b>Oturum Başkanı:</b> Nafiz Kahraman</p>
	<p><b>Numerical and Experimental Investigation of the Effect of Diesel Injector Nozzle Geometry on Coking Phenomena and Engine Performance Parameters</b> O. Özener, A. Ergenç, <u>Alper Kaya</u>, V. Gazi</p>	<p><b>Thermal Enhancement of the Combustion Process via Gliding Arc Plasma Assistance</b> <u>Ernest Bykov</u></p>
	<p><b>Analysis of Emissions of Low Temperature Combustion in a Diesel Engine According to the Combustion Process and Modeling of N2O Emissions</b> Onur Gezer, Cihan Büyük, <u>Orkun Özener</u>, Muammer Özkan</p>	<p><b>Flame Characteristics in Plasma-Assisted Combustion Of H2 Enriched NH3/CH4 Blends</b> <u>Ignas Ambrazevicius, Rolandas Paulauskas</u></p>
	<p><b>Advanced Combustion Optimization Applications in Diesel Engines</b> <u>Kenan Enes Aydın</u>, E. Aras</p>	<p><b>Investigation of Methane Combustion Characteristics in a Non-premixed Model Burner Under Colorless Distributed Combustion Conditions</b> <u>Wameedh Saleh Hadı Al</u>, E. Yıldırım, S. Karyeyen</p>
	<p><b>Investigation of Effect of Coating Thickness and Operating Temperatures Changes Against DLC Coating Delamination for Diesel Injection Systems</b> <u>Alper Kaya</u>, M. Altın</p>	<p><b>The Effect of the Chemical Mechanism and Progress Variable Definition on the LES/FGM Modeling of Spray Flame</b> <u>Onur Utku Çağlar</u>, H. Türkeri, M. Muradoğlu</p>
<p><b>Amonyak ve Hidrojen Karışımının Yanma Davranışlarının Emisyon Azaltımı ve Endüstriyel Uygulamalar İçin Numerik Olarak İncelemesi</b></p>	<p><b>Effects Of Colorless Distributed Combustion (Cdc) Technology On The Combustion And Emission Behaviors Of Ammonia/Hydrogen/Air Flame: A</b></p>	

# **FULL TEXTS**

## FLAME CHARACTERISTICS IN PLASMA-ASSISTED COMBUSTION OF H<sub>2</sub> ENRICHED NH<sub>3</sub>/CH<sub>4</sub> BLENDS

Ignas Ambrazevicius<sup>1</sup> and Rolandas Paulauskas<sup>2</sup>

1. Laboratory of Combustion Processes, Lithuanian Energy Institute, Kaunas, Lithuania, LT-44403, email: [Ignas.Ambrazevicius@lei.lt](mailto:Ignas.Ambrazevicius@lei.lt)
2. Laboratory of Combustion Processes, of Lithuanian Energy Institute, Kaunas, Lithuania, LT-44403, email: [Rolandas.Paulauskas@lei.lt](mailto:Rolandas.Paulauskas@lei.lt)

### Abstract

The European gas market is transitioning from natural gas to renewable gases to enhance climate safety and energy security. Hydrogen and ammonia are central to this transition, offering sustainable alternatives to methane. Hydrogen, a zero-emission fuel, can be produced via electrolysis using renewable energy or from natural gas with carbon capture. Ammonia, synthesized from hydrogen and nitrogen, serves as an energy carrier and storage medium. This research investigates the combustion characteristics and efficiency of hydrogen-enriched NH<sub>3</sub>/CH<sub>4</sub> blends using non-thermal plasma assistance. The experiments were conducted using a fully premixed gas burner with a thermal power of 1,33 kW. Non-thermal plasma was produced with high voltage and high frequency generator at 120 kHz and 8,33 kV. Time-resolved chemiluminescence data for OH\* and NH<sub>2</sub>\* were collected using an ICCD camera with corresponding filters, alongside measurements from MIR emission spectroscopy and a thermal irradiance flux meter. Experimental results showed that non-thermal plasma increased flame stability and enhanced infrared radiation. The highest adiabatic flame temperature was observed with an 80% methane and 20% hydrogen mixture, reaching 1442 °C without plasma and 11459 °C with plasma. Infrared radiation intensity increased by 13% for ammonia-hydrogen mixtures under plasma assistance. Heat flux measurements indicated a significant 15% increase for the 70% ammonia and 20% hydrogen blend. These findings suggest plasma-assisted combustion can enhance the efficiency and stability of low-carbon fuel mixtures, promoting their integration into existing infrastructures while reducing greenhouse gas emissions.

*Keywords:* Hydrogen, Ammonia, Plasma-assisted combustion, Renewable gases, Flame stability, Combustion efficiency, Infrared radiation, Heat flux

### INTRODUCTION

The European gas market is undergoing a significant transition from traditional natural gas to renewable gases, driven by climate saving reasons and energy security concerns. Historically reliant on methane imports, Europe is now exploring sustainable alternatives like hydrogen and ammonia.

Hydrogen, a zero-emission fuel, is central to this transition. Produced via electrolysis using renewable energy (green hydrogen) or from natural gas with carbon capture (blue hydrogen), it can be integrated into the existing gas grid [1]. Blending hydrogen with natural gas reduces emissions and

leverages current infrastructure. The European hydrogen strategy aims to scale hydrogen use across sectors. Furthermore, ammonia, synthesized from hydrogen and nitrogen, serves as an energy carrier and storage medium. It can be transported easily and used directly as fuel or converted back into hydrogen. Ammonia-methane blends offer a transitional solution, utilizing existing infrastructure while reducing greenhouse gas emissions [2]. Blending renewable gases with methane is practical, minimizing infrastructure costs and reducing emissions. However, the specific blending ratios must be carefully managed to mitigate the technical issues [3].

While the transition to renewable gases is promising, several technical challenges must be addressed, particularly in gas burners. One significant issue is the lower radiation heat release during combustion. Hydrogen and ammonia flames tend to have lower emissivity than methane, leading to less radiant heat transfer. This can affect the performance of gas burners designed for methane, potentially requiring redesign or modification to achieve efficient combustion and heat distribution [4]. Another challenge is the flame speed and stability. Hydrogen has a higher flame speed than methane, which can result in increased wear and tear on burner components and necessitate changes in burner design to ensure safe and stable combustion. Ammonia combustion, on the other hand, can produce nitrogen oxide ( $\text{NO}_x$ ) emissions, which require effective mitigation strategies such as selective catalytic reduction (SCR) systems to comply with environmental standards [5].

These technical problems can be addressed with plasma-assisted combustion technology, specifically using non-thermal gliding arc plasma. This advanced technology enhances the combustion process by generating reactive species that improve flame stability and increase combustion efficiency [6]. The nonthermal gliding arc plasma can significantly enhance the radiation heat release, overcoming the lower emissivity of hydrogen and ammonia flames [7].

Additionally, plasma-assisted combustion can reduce emissions by promoting complete and efficient combustion, thus mitigating one of the primary environmental concerns associated with ammonia. This technology also helps achieve lower ignition temperatures and maintain stable combustion at a wide range of fuel mixtures and flow rates, addressing the challenges posed by the higher flame speed of hydrogen and stability issues. Plasma-assisted combustion technology provides a robust solution to ensure efficient and stable combustion of these blends [8].

## MATERIAL AND METHODS

The experiments were performed using a fully premixed gas burner with a thermal power of 1.33 kW. Non-thermal plasma was produced using a Redline Technology G2000 generator, operating at a constant frequency of 120 kHz and 8,33 kV voltage. Time resolved chemiluminescence data for  $\text{OH}^*$  and  $\text{NH}_2^*$  were collected with ICCD camera

using different filters, alongside measurements from MIR (2000–5500 nm) emission spectroscopy and thermal irradiance flux meter.

## Gas Burning Stand

The experimental gas burning stand is shown in Figure 1. The plasma-assisted burner is made of stainless steel 20 mm outer diameter conical electrode connected to a high-voltage line and the ground electrode is a cylindrical body with internal diameter of 22 mm, made of same material. For flame stabilisation and visual observation upper part of burner is made of quartz glass tube.

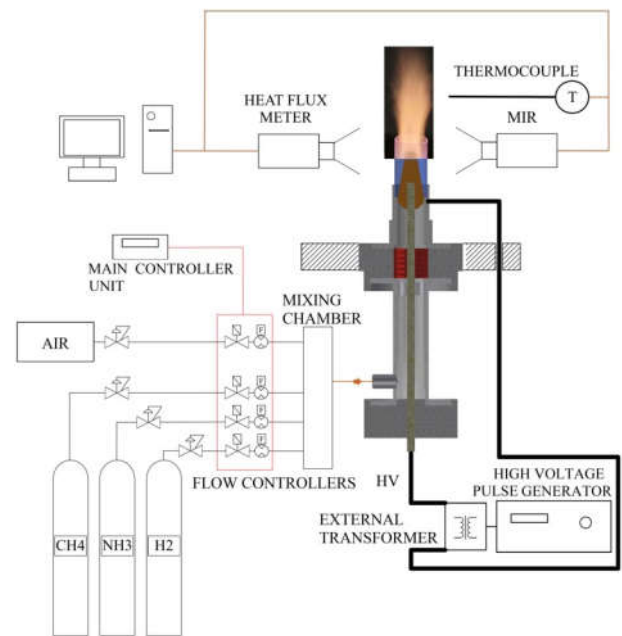


Figure 1. Experimental stand

Different gas proportions were introduced into the mixing chamber together with compressed air using mass flow controllers. After the mixing chamber the gas mixture flows into the burner main body, where a static mechanical swirler with a  $40^\circ$  flow exit angle creates a swirling motion, enhancing fuel and oxidizer mixing for efficient combustion and flame stabilization. The swirling flow moves through the burner cavity to the narrowest point between the electrodes, where an arc forms. This arc extends along the electrodes by gas flow force, elongating until it extinguishes or short-circuits, covering the gas exhaust channel with plasma arcs and creating a rotating gliding arc plasma.

Combustion air, initially supplied by the compressor at 1,5 bar pressure, passed through a silica gel drying apparatus to remove moisture, and then regulated by a flow controller before enters the mixing chamber. Combustible gases (ammonia,

methane, hydrogen) were supplied from dedicated cylinders. Each gas was routed through a pressure regulator to maintain 2–3 bar pressure, then fed into individual flow controllers for precise regulation. These controlled flows were directed into the mixing chambers to achieve a homogeneous mixture for optimal combustion.

Gas flow rates were precisely managed using a Brooks Instruments MFC unit (Brooks 0254) and controlled via a personal computer. This setup included four mass flow controllers: three for combustible gases and one for compressed air. These controllers maintained the flow according to set values, ensuring consistent combustion performance by adjusting the fuel-to-air equivalence ratio.

A high voltage plasma generator G2000 (Redline Technologies), with a maximum voltage of 8,33 kV and a frequency range of 0–500 kHz, was used to create the plasma discharge. Experiments were conducted using a 200 V (6,6 kV after the transformer) voltage and a frequency of 120 kHz, based on scientific literature [9] indicating these values are optimal for combustion optimization with non-thermal plasma.

Due to the aerodynamic properties of the fixed swirler, varying gas compositions result in different flow velocities. Consequently, the swirling motion can influence flame stability and non-thermal plasma behaviour. At low gas flows, the gliding arc can become unstable, forming long, non-rotating arcs that disrupt active species generation and flame stability. To address this issue, permanent neodymium ring magnets were introduced.



Figure 2. Plasma stabilisation with permanent magnets

As shown in Figure 2, without the magnets, there is no gliding arc rotation at low flow speeds. However, with the magnets in place, the same gas flow produces a uniform gliding arc surface due to Lorentz forces. These magnets were used to stabilize the gliding arc plasma, although no

detailed integration between the magnets and plasma was investigated.

### Luminous and non-luminous emission spectroscopy and thermal irradiance metering

The entire combustion process was observed using an advanced optical system designed to analyse the spatial distribution of excited species  $\text{OH}^*$  and  $\text{NH}_2^*$  within the flame at atmospheric pressure. Flame images were captured using an ICCD (Intensified Charge Coupled Device) camera, specifically the Andor iStar DH734.

The non-luminous emission spectroscopy was conducted using a 2000–5000 nm spectrometer (NLIR S2050–400). This spectrometer, referred to as Mid-IR spectroscopy, The spectrometer was controlled using NLIR spectroscopy software, and spectra were obtained by averaging 30 scans.

For the thermal irradiance measurement, the water-cooled thermopile SBG01 heat flux sensor was positioned at the same height as the NLIR spectrometer and 80 mm from the flame centre. This Gardon and Schmidt-Boelter type sensor, equipped with a black absorber, measures heat flux up to  $50 \text{ kW/m}^2$ . No additional optical filter was used to filter different irradiance wavelengths. The sensor generated an output voltage proportional to the incoming thermal irradiance, which was recorded using a Rigol DM 3068 digital multimeter connected to a personal computer.

### Methodology for conducting combustion experiments

Experiments were conducted with various gas compositions and different fuel-to-air ratios. Initially, calibration with only methane gas ensured measurement accuracy. Subsequent tests used different gas mixtures: methane and ammonia, methane and hydrogen, and hydrogen and ammonia with some methane, incorporating up to 20–30% hydrogen.

Gas mixtures and flow rates were calculated to maintain a constant thermal combustion power of 1,33 kW. Detailed stoichiometric calculations, in accordance with the EN12953:11 standard, determined the required combustion air, gas flow rates, adiabatic flame temperatures, and calorific values. The results of these calculations are shown in Table 1.

Table 1. Gas mixture combustion calculation results

Parameter	Units	100%CH <sub>4</sub>	80%CH <sub>4</sub> + 20%NH <sub>3</sub>	80%CH <sub>4</sub> + 20%H <sub>2</sub>	10%CH <sub>4</sub> + 70%NH <sub>3</sub>
Fuel to air ratio	–	0,81	0,81	0,81	0,81
Adiabatic flame temperature	°C	1748	1732	1762	1670
Gas calorific value	kJ/N m <sup>3</sup>	35833	31578	30863	15797
Gas flow	NL/m in	2,17	2,47	2,53	4,93
Thermal power of the burner	kW	1,3	1,3	1,3	1,3

It was observed that the highest adiabatic temperatures calculated with a mixture of 80% methane and 20% hydrogen, while the lowest temperatures were calculated with a mixture of 70% ammonia and 20% hydrogen. In the ammonia–hydrogen mixture, 10% methane was introduced to stabilize combustion. For future experiments, methane will not be used.

For a better understanding of the thermal irradiance properties of these gas mixtures, the flue gas composition was also calculated.

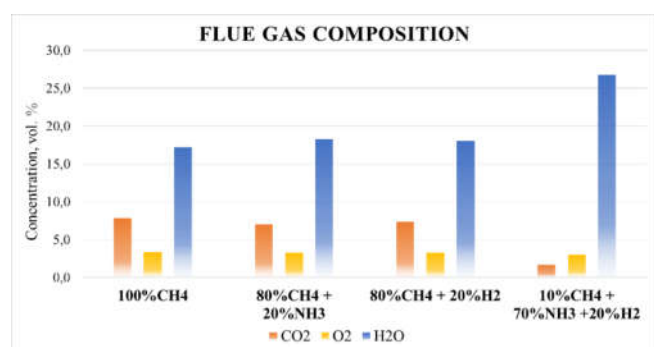


Figure 3. Calculated flue gas composition

Figure 3 shows the flue gas composition for different gas mixtures. It can be observed that the concentration of triatomic gases, such as H<sub>2</sub>O (water vapour) and CO<sub>2</sub> (carbon dioxide), varies across the mixtures. For methane, methane and hydrogen, hydrogen and ammonia mixtures, there is a modest variation in water vapour and carbon dioxide concentrations. However, for the

ammonia–hydrogen mixture, the H<sub>2</sub>O (water vapour) concentration is significantly higher. The influence of this increased water vapour concentration on irradiated heat flux was analysed during the experiments.

## RESULTS

The main goal of these experiments is to investigate the thermal irradiation of flames from different gas mixtures and analyse how varying compositions influence heat flux, distribution of excited OH\* and NH<sub>2</sub>\* species, infrared spectrum characteristics, and flame temperature. Non–thermal plasma assisted combustion could impact the infrared spectrum by enhancing the emission of IR radiation through the formation of CO<sub>2</sub> and H<sub>2</sub>O, which have strong IR absorption and emission bands. Increased flame temperatures and the generation of intermediate species like OH\* and NH<sub>2</sub>\* could further enhance thermal radiation.

### Flame characteristics

In Figure 4, various images illustrate flames without plasma assistance, maintaining identical fuel–to–air ratios. These images were captured to compare flame stability, shapes, and colours with and without non–thermal plasma assistance. The 100% methane flame exhibits a bright blue colour and a slight V shape due to the swirler's influence. Methane–ammonia mixtures produce a yellow flame, lengthening the flame itself. Methane mixtures with 20% hydrogen display bright red flames with distinct methane and hydrogen combustion zones. The 70% ammonia and 20% hydrogen mixture results in the longest flame, characterized by a laminar flow pattern.

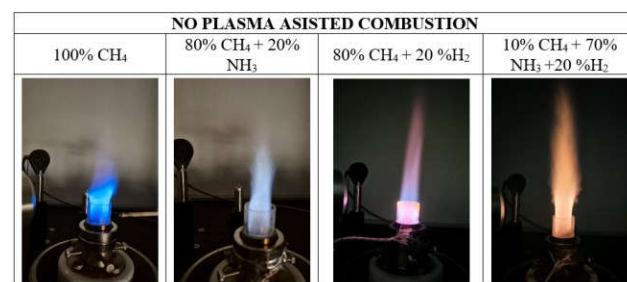


Figure 4. No plasma–assisted flame images

The injection of hydrogen into gas mixtures significantly impacts flame characteristics. Hydrogen enhances combustion by increasing flame temperature and speed, resulting in brighter and more intense flame colours. It also helps

stabilize the flame, especially in fuel-lean conditions, due to its high diffusivity and reactivity.

With non-thermal plasma assistance, the flame exhibited increased intensity and enhanced stability. In the case of a mixture comprising 70% ammonia and 20% hydrogen with low fuel-to-air ratios, the flame became unstable and tended to extinguish under extremely lean conditions. However, with the introduction of plasma assistance, this mixture combusted efficiently without any issues.

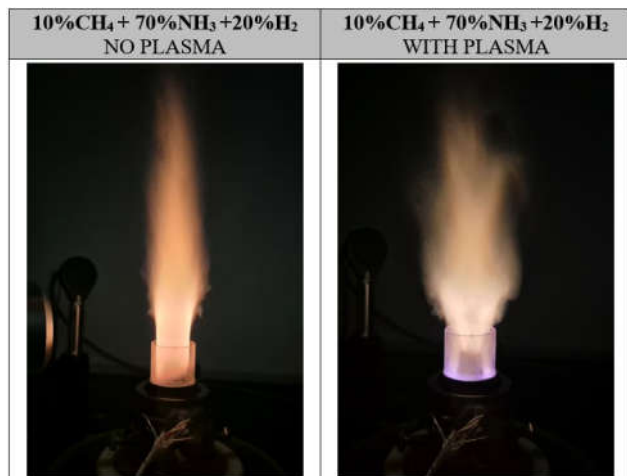


Figure 5. Plasma influence on flames

This phenomenon is shown in Figure 5. Using non-thermal plasma, the flame intensity increased, the flame shape became shorter and more turbulent, a distinct V shape was formed. This demonstrates that non-thermal plasma can significantly improve the combustion process, ensuring stable and complete combustion even in challenging fuel-lean scenarios.

In addition, the flame temperatures were measured using an R-type thermocouple. A 100% methane flame with a fuel-to-air ratio of 0.81 was used as the reference point. The measured flame temperature was 1307°C without plasma assistance and 1316°C with non-thermal plasma assistance. Despite the visual observation of a more intense and uniform flame with plasma assistance, the temperature increase for this mixture was not significant. The difference between the calculated adiabatic flame temperature and the measured temperature can be attributed to the lack of heat insulation in the combustion chamber, which resulted in substantial heat losses.

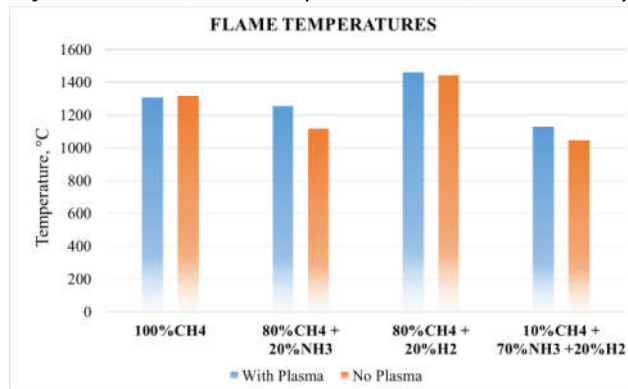


Figure 6. Flame temperatures

The distribution of flame temperatures with and without non-thermal plasma assistance is shown in Figure 6 for different gas mixtures. Due to the lower volumetric calorific values of ammonia and hydrogen, it was expected that ammonia gas mixtures would reach lower flame temperatures. This expectation was confirmed for the 80% methane and 20% ammonia, 70% ammonia and 20% hydrogen mixtures. As predicted from adiabatic temperature calculations and calorific values, the 70% ammonia and 20% hydrogen mixture exhibited the lowest flame temperatures. Conversely, the 80% methane and 20% hydrogen mixture reached the highest flame temperatures.

### Radiative flame characteristics

Major combustion products such as carbon dioxide (CO<sub>2</sub>) and water vapour (H<sub>2</sub>O) exhibit strong IR absorption and emission due to their vibrational and rotational transitions [10]. CO<sub>2</sub> shows strong. In references [11], it is noted that CO<sub>2</sub> emits at wavelengths around 2000 nm and 4400 nm, H<sub>2</sub>O emits between 1800 and 2000 nm and coincides with CO<sub>2</sub> emissions at approximately 2800 nm. Recent studies also indicate that a peak intensity at 2500 nm is attributed to H<sub>2</sub>O, with. Additionally, Henrion et al. [12] found that the highest intensities are at wavelengths of 4300–4500 nm due to CO<sub>2</sub> emissions.

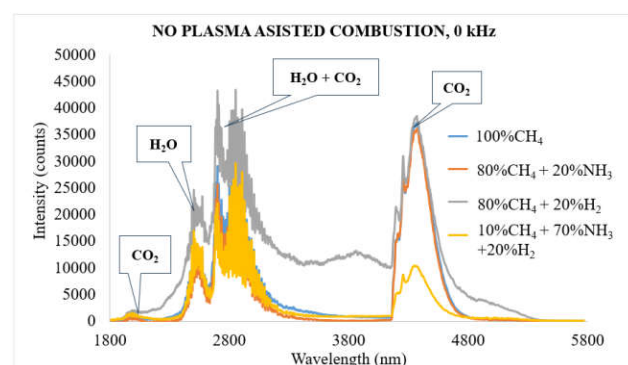


Figure 7. Infrared radiation spectra for different gas mixtures with no plasma

Figure 7 displays the IR spectra of gas mixtures without plasma assistance, highlighting CO<sub>2</sub> and H<sub>2</sub>O as the primary thermal emitters at different wavelengths [13]. The infrared (IR) spectral analysis of the infrared (IR) spectral analysis of H<sub>2</sub>O and CO<sub>2</sub> bands revealed distinct variations in intensity based on different gas mixtures. The highest IR intensities for the H<sub>2</sub>O and mixed H<sub>2</sub>O + CO<sub>2</sub> spectra were observed in the mixture containing 80% methane and 20% hydrogen. In contrast, the mixture of 70% ammonia and 20% hydrogen exhibited lower IR intensities.

Specifically, for the CO<sub>2</sub> alone bands, the mixture of 70% ammonia and 30% hydrogen showed the lowest intensity, likely due to the low carbon content present in this gas mixture. These findings are particularly significant given the critical role of CO<sub>2</sub> in the radiative properties of flue gases.

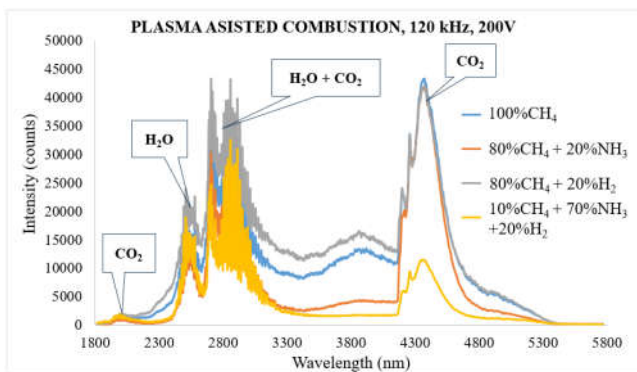


Figure 8. Infrared radiation spectra for different gas mixtures with plasma

In comparison, the same gas mixtures were used to analyse IR spectrum intensities under the influence of a nonthermal plasma in Figure 8. The application of nonthermal plasma significantly increased the IR intensities across all observed bands. For the mixture of 80% methane and 20% hydrogen, the IR intensities for both H<sub>2</sub>O and the mixed H<sub>2</sub>O + CO<sub>2</sub> spectra showed a notable enhancement when subjected to the nonthermal plasma. Similarly, the mixture of 70% ammonia and 20% hydrogen, which initially exhibited lower IR intensities, also demonstrated a marked increase in intensity.

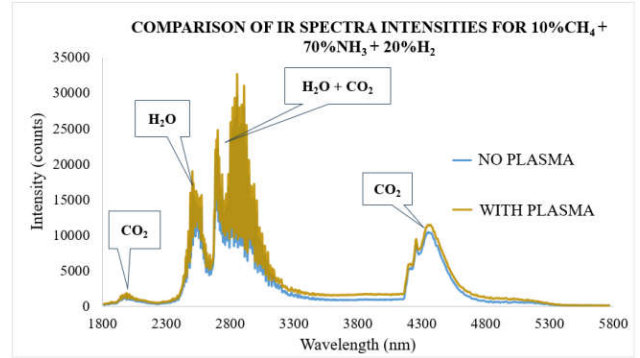


Figure 9. Infrared radiation spectra ammonia hydrogen mixture with and without plasma

In Figure 9, a comparison of IR spectrum intensities for a 70% ammonia and 20% hydrogen mixture are shown in one graph. Due to the low carbon content, introducing 10% methane resulted in the highest intensities on the H<sub>2</sub>O and mixed H<sub>2</sub>O + CO<sub>2</sub> bands and the lowest in CO<sub>2</sub>-only bands. When nonthermal plasma was applied, a general spectrum intensity was increased by 13%. The same phenomenon was noted for the CO<sub>2</sub> band alone, indicating that for carbon-free gas mixtures, additional CO<sub>2</sub> could enhance spectral intensities. However, more detailed experimental studies on the effects of additional CO<sub>2</sub> gas injection are needed to optimize these observations and fully understand the underlying mechanisms.

To better understand the influence of plasma on flame characteristics, spatial emissions of OH\* and NH<sub>2</sub>\* from flame chemiluminescence were observed using an ICCD camera. The data were converted to flame images with equal intensity scales for these species, employing an NH<sub>2</sub>\* filter for gas mixtures containing ammonia and OH\* for all mixtures. In Figure 10, the 70% ammonia and 20% hydrogen mixture are shown without plasma assistance using the NH<sub>2</sub>\* filter. The flame temperature and speed were lower, resulting in a longer, laminar-like flow flame shape.

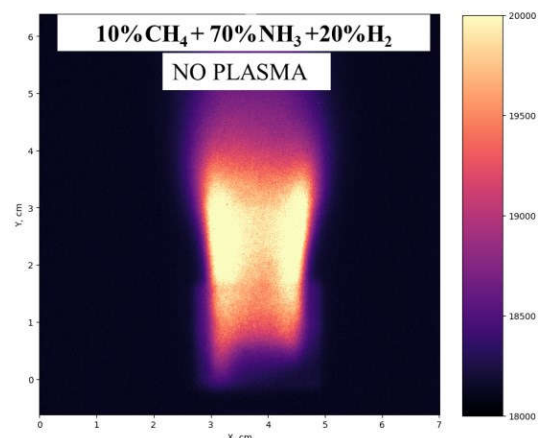


Figure 10. Flame images with  $\text{NH}_2^*$  bandpass filter with no plasma assistance

Additionally, Figure 11 illustrates the 70% ammonia and 20% hydrogen mixture using the  $\text{NH}_2^*$  filter with plasma assistance. Plasma-assisted combustion widened the flame and enhanced flame stability, with increased spatial emissions observed at higher frequencies. It was also observed that the flame core is significantly higher compared to combustion without plasma. On average, with plasma assistance, the flame core was 10 mm higher for mentioned gas mixture and 0,81 fuel-to-air ratio. These results indicate a positive thermal and kinetic effect of plasma, expanding the flame-covered zone and intensifying  $\text{OH}^*$  and  $\text{NH}_2^*$  emissions.

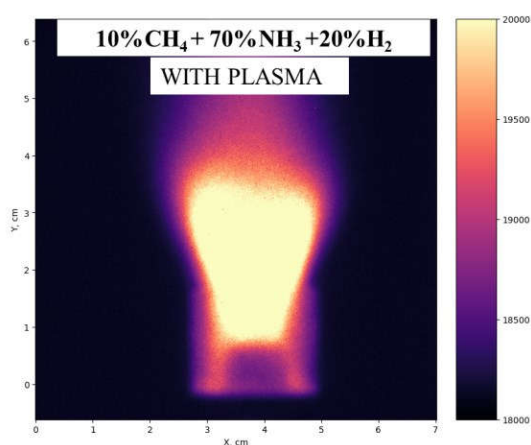


Figure 11. Flame images with  $\text{NH}_2^*$  bandpass filter with plasma assistance

Finally, the heat flux from the flame was measured for the different gas mixtures. Figure 12 shows the distribution of heat flux irradiated from the gas burner flames, indicating that the highest heat flux was from the 80% methane and 20% hydrogen mixture, while the lowest was from the 70% ammonia and 20% hydrogen mixture. These results, combined with measured IR spectra and flame temperature measurements, underscore the high importance of  $\text{CO}_2$  gas concentration in flue gases for different gas mixtures.

The use of nonthermal plasma increased the heat flux values, with the highest increase observed for 100% methane and progressively lower increments for methane-ammonia and ammonia-hydrogen mixtures. Despite this, for the low-carbon mixture of 70% ammonia and 20% hydrogen, the increase in heat flux intensity was 15%. This is a significant increment for mixtures with low carbon content, highlighting the efficacy of plasma assistance in

enhancing combustion properties even in low-carbon scenarios.

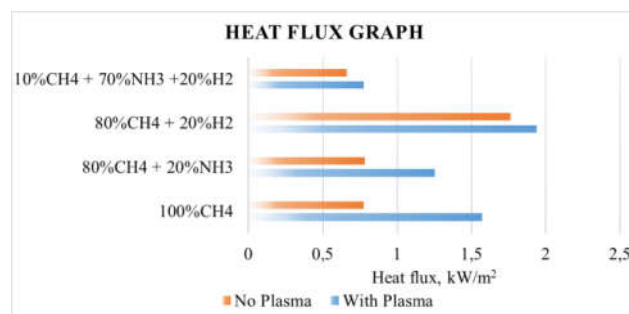


Figure 12. Measured flame heat flux with and without plasma assistance

## CONCLUSIONS

The experiments were made to investigate the thermal irradiation and flame characteristics of  $\text{H}_2$  - enriched  $\text{NH}_3/\text{CH}_4$  blends using plasma-assisted combustion. Various mechanisms enhance IR radiation in plasma-assisted combustion. Higher flame temperatures resulting from plasma-assisted combustion increase IR radiation due to the Stefan-Boltzmann law, which states that radiative heat flux is proportional to the fourth power of temperature. Non-thermal plasma promotes the formation of intermediate species like  $\text{OH}^*$ ,  $\text{CH}^*$ , and other radicals, which influence the combustion process and enhance IR radiation indirectly by stabilizing the flame and increasing temperature.

Without plasma assistance, methane flames exhibited a bright blue colour, while methane-ammonia mixtures produced yellow flames with longer shapes. Methane-hydrogen mixtures displayed bright red flames, with the hydrogen enhancing combustion by increasing flame temperature and speed. The 70% ammonia and 20% hydrogen mixture resulted in the longest flame, characterized by a laminar flow pattern.

Non-thermal plasma significantly improved flame stability and intensity. Plasma-assisted flames were more turbulent, shorter, and displayed a distinct V - shape. The flame temperatures increased slightly with plasma assistance. For a 100% methane flame, the temperature increased from 1307 °C to 1316 °C, for other gas mixtures the temperature increment was about 100 K. Flame images captured with  $\text{NH}_2^*$  filters showed that plasma-assisted combustion widened the flame and enhanced stability, with increased spatial emissions of  $\text{OH}^*$  and  $\text{NH}_2^*$ .

Non-thermal plasma enhanced the IR intensities across all gas mixtures. For the 80% methane and 20% hydrogen mixture, IR intensities for H<sub>2</sub>O and CO<sub>2</sub> spectra increased notably. The 70% ammonia and 20% hydrogen mixture, which initially exhibited lower IR intensities, also showed an increase with plasma assistance. The highest IR intensities for H<sub>2</sub>O and mixed H<sub>2</sub>O + CO<sub>2</sub> spectra were observed in the 80% methane and 20% hydrogen mixture. The highest heat flux was observed in the 80% methane and 20% hydrogen mixture, while the lowest was in the 70% ammonia and 20% hydrogen mixture. With the non-thermal plasma the heat flux values increased with a 15% for the low-carbon mixture of 70% ammonia and 20% hydrogen. Plasma-assisted combustion enhanced flame temperatures and the generation of intermediate species, contributing to improved combustion efficiency and increased IR radiation and demonstrating potential for practical applications in sustainable energy systems.

## REFERENCES

- [1] The European Hydrogen Backbone (EHB) initiative, <https://www.ehb.eu/> (viewed: 18 06 2024)
- [2] H. Kobayashi, A. Hayakawa, K. Kunkuma, A. Somarathne, C. Ekenechukwu. *Science and technology of ammonia combustion, Proceedings of the Combustion Institute*, Volume 37, Issue 1. 2019 <https://doi.org/10.1016/j.proci.2018.09.029>
- [3] W. Guanqing, H. Longfei, T. Huaxin T, Z. Hang, Ch. Xiangxiang, X. Jiangrong, *Stable lean co-combustion of ammonia/methane with air in a porous burner*, *Applied Thermal Engineering*, Volume 248, Part A, 2024 <https://doi.org/10.1016/j.applthermaleng.2024.123092>
- [4] R. Skvorčinskienė, N. Striūgas, K. Zakarauskas, R. Paulauskas, *Combustion of waste gas in a low-swirl burner under syngas and oxygen enrichment*, *Fuel*, Volume 298, 2021 <https://doi.org/10.1016/j.fuel.2021.120730>
- [5] W. Yong, G. Mingyan, L. Shuanglong, W. Xin, H. Xiangyong, L. Qifu, *Study on the NO<sub>x</sub> formation of propane/ammonia co-combustion with a swirl burner*, *Applications in Energy and Combustion Science*, Volume 17, 2024, <https://doi.org/10.1016/j.jaecs.2023.100242>.
- [6] E. Bykov, A. Jančauskas, R. Paulauskas, K. Zakarauskas, N. Striūgas, *Plasma assisted combustion of different biogas mixtures in low swirl burner*, *Fuel*, Volume 368, 2024 <https://doi.org/10.1016/j.fuel.2024.131602>
- [7] J. Zembi, V. Cruccolini, F. Mariani, R. Scarcelli, M. Battistoni. *Modeling of thermal and kinetic processes in non-equilibrium plasma ignition applied to a lean combustion engine*. *Appl Therm Eng.* 2021 <https://doi.org/10.1016/j>
- [8] N. Striūgas, A. Tamošiūnas, L. Marcinauskas, R. Paulauskas, K. Zakarauskas, R. Skvorčinskienė, *A sustainable approach for plasma reforming of tail biogas for onsite syngas production during lean combustion operation*, *Energy Conversion and Management*, Volume 209, 2020 <https://doi.org/10.1016/j.enconman.2020.112617>
- [9] E. Bykov, N. Striūgas, R. Paulauskas *Emission Spectroscopy of CH<sub>4</sub>/CO<sub>2</sub> Mixtures Processed in a Non-Thermal Plasma Augmented Burner Catalysts* 12, No. 12: 1540. 2022 <https://doi.org/10.3390/catal12121540>
- [10] D. Ottesen, D. Stephenson. *Fourier Transform Infrared (FTIR) Measurements In Sooting Flames*. California 1981
- [11] E. Plyler, C. Humphreys. *Infrared emission spectra of flames*. National Bureau of Standards 1948
- [12] L. Henrion, V. Sick, D. C. Haworth, *A detailed experimental and modelling comparison of molecular radiative heat loss in a spark-ignition engine*, *Combustion and Flame*, Volume 241, 2022 <https://doi.org/10.1016/j.combustflame.2022.112083>
- [13] G. Faeth, J. Gore, S-M. Jeng. *Spectral and total radiation properties of turbulent carbon monoxide/air diffusion flames*, Michigan 1987 <https://doi.org/10.2514/3.9627>